

# New Clock Comparison Searches for Lorentz and CPT Violation

Ronald L. Walsworth, David Bear, Marc Humphrey,  
Edward M. Mattison, David F. Phillips, Richard E. Stoner,  
and Robert F. C. Vessot

*Harvard-Smithsonian Center for Astrophysics  
Cambridge, MA 02138, U.S.A.*

*to appear in the Proceedings of the 3rd International Symposium  
on Symmetries in Subatomic Physics*

**Abstract.** We present two new measurements constraining Lorentz and CPT violation using the  $^{129}\text{Xe}/^3\text{He}$  Zeeman maser and atomic hydrogen masers. Experimental investigations of Lorentz and CPT symmetry provide important tests of the framework of the standard model of particle physics and theories of gravity. The two-species  $^{129}\text{Xe}/^3\text{He}$  Zeeman maser bounds violations of CPT and Lorentz symmetry of the neutron at the  $10^{-31}$  GeV level. Measurements with atomic hydrogen masers provide a clean limit of CPT and Lorentz symmetry violation of the proton at the  $10^{-27}$  GeV level.

## INTRODUCTION

Lorentz symmetry is a fundamental feature of modern descriptions of nature. Lorentz transformations include both spatial rotations and boosts. Therefore, experimental investigations of rotation symmetry provide important tests of the framework of the standard model of particle physics and single-metric theories of gravity [1].

In particular, the minimal  $\text{SU}(3) \times \text{SU}(2) \times \text{U}(1)$  standard model successfully describes particle phenomenology, but is believed to be the low energy limit of a more fundamental theory that incorporates gravity. While the fundamental theory should remain invariant under Lorentz transformations, spontaneous symmetry-breaking could result at the level of the standard model in violations of local Lorentz invariance (LLI) and CPT (symmetry under simultaneous application of Charge conjugation, Parity inversion, and Time reversal) [2].

Clock comparisons provide sensitive tests of rotation invariance and hence Lorentz symmetry by bounding the frequency variation of a given clock as its orientation changes, e.g., with respect to the fixed stars [3]. In practice, the most precise limits are obtained by comparing the frequencies of two co-located clocks

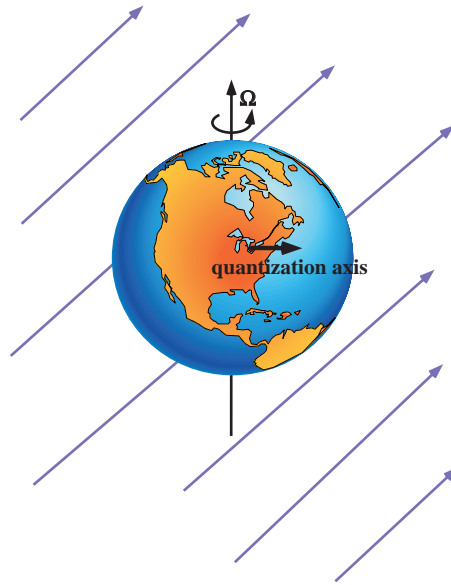


**FIGURE 1.** Bounds on LLI and CPT violation can be obtained by comparing the frequencies of clocks as they rotate with respect to the fixed stars. The standard model extension described in [3,9–17] admits Lorentz-violating couplings of noble gas nuclei and hydrogen atoms to expectation values of tensor fields. (Some of these couplings also violate CPT.) Each of the tensor fields may have an unknown magnitude and orientation in space, to be limited by experiment. The background arrows in this figure illustrate one such field.

as they rotate with the Earth (see Fig. 1). Atomic clocks are typically used, involving the electromagnetic signals emitted or absorbed on hyperfine or Zeeman transitions.

We report results from two new atomic clock tests of LLI and CPT:

- (1) Using a two-species  $^{129}\text{Xe}/^3\text{He}$  Zeeman maser [4–6] we placed a limit on CPT and LLI violation of the neutron of nearly  $10^{-31}$  GeV, improving by more than a factor of six on the best previous measurement [7,8].
- (2) We employed atomic hydrogen masers to set an improved clean limit on LLI/CPT violation of the proton, at the level of nearly  $10^{-27}$  GeV.

## MOTIVATION

Our atomic clock comparisons are motivated by a standard model extension developed by Kostelecký and others [3,9–17]. This theoretical framework accommodates possible spontaneous violation of local Lorentz invariance (LLI) and CPT symmetry, which may occur in a fundamental theory combining the standard model with gravity. For example, this might occur in string theory [18]. The standard

model extension is quite general: it emerges as the low-energy limit of any underlying theory that generates the standard model and contains spontaneous Lorentz symmetry violation [19]. The extension retains the usual gauge structure and power-counting renormalizability of the standard model. It also has many other desirable properties, including energy-momentum conservation, observer Lorentz covariance, conventional quantization, and hermiticity. Microcausality and energy positivity are expected.

This well-motivated theoretical framework suggests that small, low-energy signals of LLI and CPT violation may be detectable in high-precision experiments. The dimensionless suppression factor for such effects would likely be the ratio of the low-energy scale to the Planck scale, perhaps combined with dimensionless coupling constants [3,9–19]. A key feature of the standard model extension of Kostelecký *et al.* is that it is at the level of the known elementary particles, and thus enables quantitative comparison of a wide array of tests of Lorentz symmetry. In recent work the standard model extension has been used to quantify bounds on LLI and CPT violation from measurements of neutral meson oscillations [9]; tests of QED in Penning traps [10]; photon birefringence in the vacuum [11,12]; baryogenesis [13]; hydrogen and antihydrogen spectroscopy [14]; experiments with muons [15]; a spin-polarized torsion pendulum [16]; observations with cosmic rays [17]; and atomic clock comparisons [3]. Recent experimental work motivated by this standard model extension includes Penning trap tests by Gabrielse *et al.* on the antiproton and  $H^-$  [20], and by Dehmelt *et al.* on the electron and positron [21,22], which place improved limits on CPT and LLI violation in these systems. Also, a re-analysis by Adelberger, Gundlach, Heckel, and co-workers of existing data from the “Eöt-Wash II” spin-polarized torsion pendulum [23,24] sets the most stringent bound to date on CPT and LLI violation of the electron: approximately  $10^{-28}$  GeV [25].

## **$^{129}\text{Xe}/^3\text{He}$ MASER TEST OF CPT AND LORENTZ SYMMETRY**

The design and operation of the two-species  $^{129}\text{Xe}/^3\text{He}$  maser has been discussed in recent publications [4–6]. (See the schematic in Fig. 2.) Two dense, co-located ensembles of  $^3\text{He}$  and  $^{129}\text{Xe}$  atoms perform continuous and simultaneous maser oscillations on their respective nuclear spin 1/2 Zeeman transitions at approximately 4.9 kHz for  $^3\text{He}$  and 1.7 kHz for  $^{129}\text{Xe}$  in a static magnetic field of 1.5 gauss. This two-species maser operation can be maintained indefinitely. The population inversion for both maser ensembles is created by spin exchange collisions between the noble gas atoms and optically-pumped Rb vapor [26]. The  $^{129}\text{Xe}/^3\text{He}$  maser has two chambers, one acting as the spin exchange “pump bulb” and the other serving as the “maser bulb”. This two chamber configuration permits the combination of physical conditions necessary for a high flux of spin-polarized noble gas atoms into the maser bulb, while also maintaining  $^3\text{He}$  and  $^{129}\text{Xe}$  maser oscillations with good frequency stability:  $\sim 100$  nHz stability is typical for measurement intervals of  $\sim 1$

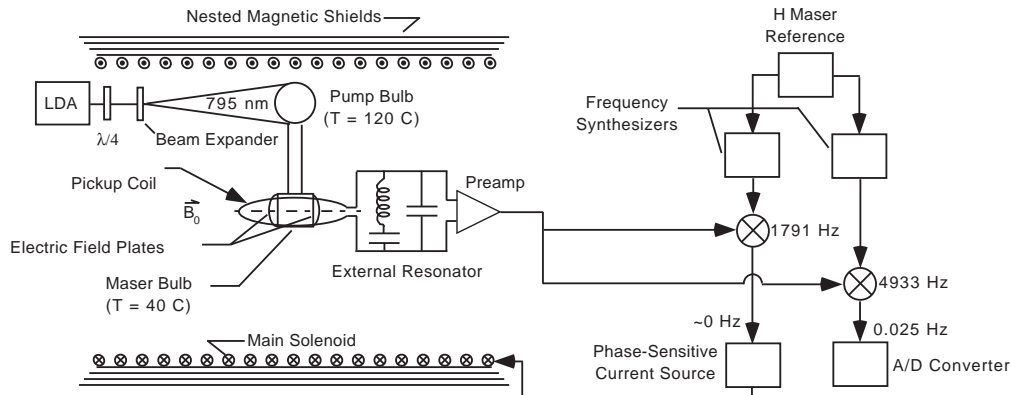


FIGURE 2. Schematic of the  $^{129}\text{Xe}/^3\text{He}$  Zeeman maser

hour [6]. (A single-bulb  $^{129}\text{Xe}/^3\text{He}$  maser does not provide good frequency stability because of the large Fermi contact shift of the  $^{129}\text{Xe}$  Zeeman frequency caused by  $^{129}\text{Xe}$ -Rb collisions [27].) Either of the noble gas species can serve as a precision magnetometer to stabilize the system's static magnetic field, while the other species is employed as a sensitive probe for LLI- and CPT-violating interactions or other subtle physical influences. (For example, we are also using the  $^{129}\text{Xe}/^3\text{He}$  maser to search for a permanent electric dipole moment of  $^{129}\text{Xe}$  as a test of time reversal symmetry; hence the electric field plates in Fig. 2.)

We search for a signature of Lorentz violation by monitoring the relative phases and Zeeman frequencies of the co-located  $^3\text{He}$  and  $^{129}\text{Xe}$  masers as the laboratory reference frame rotates with respect to the fixed stars. We operate the system with the quantization axis directed east-west on the Earth, the  $^3\text{He}$  maser free-running, and the  $^{129}\text{Xe}$  maser phase-locked to a signal derived from a hydrogen maser in order to stabilize the magnetic field. To leading order, the standard model extension of Kostelecký *et al.* predicts that the Lorentz-violating frequency shifts for the  $^3\text{He}$  and  $^{129}\text{Xe}$  maser are the same size and sign [3]. Hence the possible Lorentz-violating frequency shift in the free-running  $^3\text{He}$  maser ( $\delta\nu_{He}$ ) is given by:

$$\delta\nu_{He} = \delta\nu_{Lorentz} [\gamma_{He}/\gamma_{Xe} - 1], \quad (1)$$

where  $\delta\nu_{Lorentz}$  is the sidereal-day-period modulation induced in both noble gas Zeeman frequencies by the Lorentz-violating interaction, and  $\gamma_{He}/\gamma_{Xe} \approx 2.75$  is the ratio of gyromagnetic ratios for  $^3\text{He}$  and  $^{129}\text{Xe}$ .

We acquired 90 days of data for this experiment over the period April, 1999 to April, 2000. We reversed the main magnetic field of the apparatus every  $\sim 4$  days to help distinguish possible Lorentz-violating effects from diurnal systematic variations. In addition, we carefully assessed the effectiveness of the  $^{129}\text{Xe}$  co-magnetometer, and found that it provides excellent isolation from possible diurnally-varying ambient magnetic fields, which would not average away with field reversals. Furthermore, the relative phase between the solar and sidereal

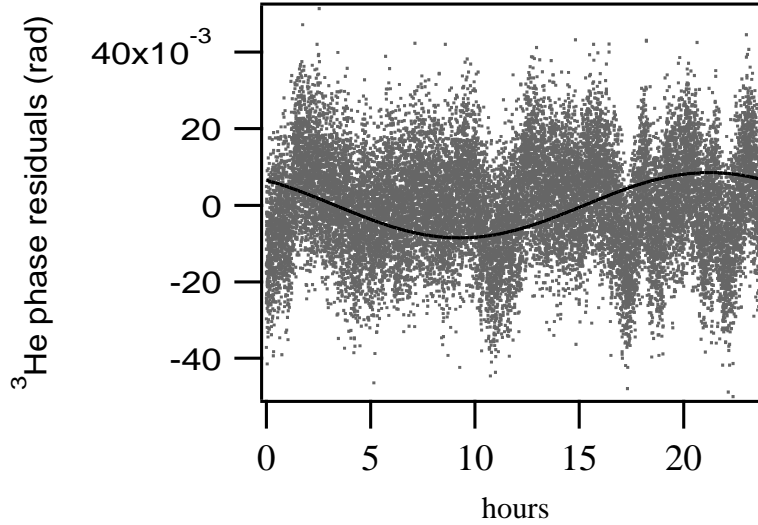


**FIGURE 3.** Typical data from the LLI/CPT test using the  $^{129}\text{Xe}/^3\text{He}$  maser.  $^3\text{He}$  maser phase data residuals are shown for one sidereal day. Larmor precession and drift terms have been removed, and the best-fit sinusoid curve (with sidereal-day-period) is displayed

day evolved about  $2\pi$  radians over the course of the experiment; hence diurnal systematic effects from any source would be reduced by averaging the results from the measurement sets.

We analyzed each day's data and determined the amplitude and phase of a possible sidereal-day-period variation in the free-running  $^3\text{He}$  maser frequency. (See Fig. 3 for an example of one day's data.) We employed a linear least squares method to fit the free-running maser phase vs. time using a minimal model including: a constant (phase offset); a linear term (Larmor precession); and cosine and sine terms with sidereal day period. For each day's data, we included terms corresponding to quadratic and maser amplitude-induced phase drift if they significantly improved the reduced  $\chi^2$  [28]. As a final check, we added a *faux* Lorentz-violating effect of known phase and amplitude to the raw data and performed the analysis as before. We considered our data reduction for a given sidereal day to be successful if the synthetic physics was recovered and there was no significant change in the covariance matrix generated by the fitting routine.

Using the 90 days of data, we found no statistically significant sidereal variation of the free-running  $^3\text{He}$  maser frequency at the level of 90 nHz (two-sigma confidence). Kostelecký and Lane report that the nuclear Zeeman transitions of  $^{129}\text{Xe}$  and  $^3\text{He}$  are primarily sensitive to Lorentz-violating couplings of the neutron, assuming the correctness of the Schmidt model of the nuclei [3]. Thus our search for a sidereal-period frequency shift of the free-running  $^3\text{He}$  maser ( $\delta\nu_{He}$ ) provides a bound to the following parameters characterizing the magnitude of LLI/CPT violations in the standard model extension:

$$\left| -3.5\tilde{b}_J^n + 0.012\tilde{d}_J^n + 0.012\tilde{g}_{D,J}^n \right| \leq 2\pi\delta\nu_{He,J}({}^{129}\text{Xe}/{}^3\text{He maser}) \quad (2)$$

Here  $J = X, Y$  denotes spatial indices in a non-rotating frame, with  $X$  and  $Y$  oriented in a plane perpendicular to the Earth's rotation axis and we have taken  $\hbar = c = 1$ . The parameters  $\tilde{b}_J^n$ ,  $\tilde{d}_J^n$ , and  $\tilde{g}_{D,J}^n$  describe the strength of Lorentz-violating couplings of the neutron to possible background tensor fields.  $\tilde{b}_J^n$  and  $\tilde{g}_{D,J}^n$  correspond to couplings that violate both CPT and LLI, while  $\tilde{d}_J^n$  corresponds to a coupling that violates LLI but not CPT. All three of these parameters are different linear combinations of fundamental parameters in the underlying relativistic Lagrangian of the standard model extension [3,9–16].

It is clear from Eqn. (2) that the  ${}^{129}\text{Xe}/{}^3\text{He}$  clock comparison is primarily sensitive to LLI/CPT violations associated with the neutron parameter  $\tilde{b}_J^n$ . Similarly, the most precise previous search for LLI/CPT violations of the neutron, the  ${}^{199}\text{Hg}/{}^{133}\text{Cs}$  experiment of Lamoreaux, Hunter *et al.* [7,8], also had principal sensitivity to  $\tilde{b}_J^n$  at the following level [3]:

$$\left| \frac{2}{3}\tilde{b}_J^n + \{\text{small terms}\} \right| \leq 2\pi\delta\nu_{Hg,J}({}^{199}\text{Hg}/{}^{133}\text{Cs}). \quad (3)$$

In this case, the experimental limit,  $\delta\nu_{Hg,J}$ , was a bound of 110 nHz (two-sigma confidence) on a sidereal-period variation of the  ${}^{199}\text{Hg}$  nuclear Zeeman frequency, with the  ${}^{133}\text{Cs}$  electronic Zeeman frequency serving as a co-magnetometer.

Therefore, in the context of the standard model extension of Kostelecký and co-workers [3], our  ${}^{129}\text{Xe}/{}^3\text{He}$  maser measurement improves the constraint on  $\tilde{b}_J^n$  to nearly  $10^{-31}$  GeV, or more than six times better than the  ${}^{199}\text{Hg}/{}^{133}\text{Cs}$  clock comparison [7,8]. Note that the ratio of this limit to the neutron mass ( $10^{-31}\text{GeV}/m_n \sim 10^{-31}$ ) compares favorably to the dimensionless suppression factor  $m_n/M_{Planck} \sim 10^{-19}$  that might be expected to govern spontaneous symmetry breaking of LLI and CPT originating at the Planck scale. We expect more than an order of magnitude improvement in sensitivity to LLI/CPT-violation of the neutron using a new device recently demonstrated in our laboratory: the  ${}^{21}\text{Ne}/{}^3\text{He}$  Zeeman maser.

## HYDROGEN MASER TEST OF CPT AND LORENTZ SYMMETRY

The hydrogen maser is an established tool in precision tests of fundamental physics [29]. Hydrogen masers operate on the  $\Delta F = 1$ ,  $\Delta m_F = 0$  hyperfine transition in the ground state of atomic hydrogen [30]. Hydrogen molecules are dissociated into atoms in an RF discharge, and the atoms are state selected via a hexapole magnet (Fig. 4). The high field seeking states, ( $F = 1$ ,  $m_F = +1, 0$ ) are focused into a Teflon coated cell which resides in a microwave cavity resonant with the  $\Delta F = 1$  transition at 1420 MHz. The  $F = 1$ ,  $m_F = 0$  atoms are stimulated to

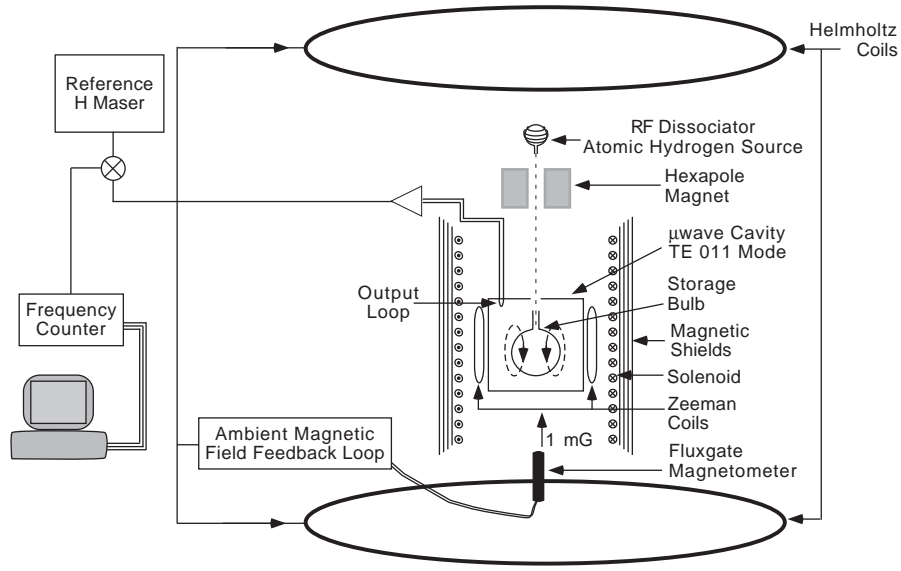


**FIGURE 4.** Schematic of the H maser in its ambient field stabilization loop.

make a transition to the  $F = 0$  state by the field of the cavity. A static magnetic field of  $\sim 1$  milligauss is applied to maintain the quantization axis of the H atoms.

The hydrogen transitions most sensitive to potential CPT and LLI violations are the  $F = 1$ ,  $\Delta m_F = \pm 1$  Zeeman transitions. In the 0.6 mG static field applied for these measurements, the Zeeman frequency is  $\nu_Z \approx 850$  Hz. We utilize a double resonance technique to measure this frequency with a precision of  $\sim 1$  mHz [31]. We apply a weak magnetic field perpendicular to the static field and oscillating at a frequency close to the Zeeman transition. This audio-frequency driving field couples the three sublevels of the  $F = 1$  manifold of the H atoms. Provided a population difference exists between the  $m_F = \pm 1$  states, the energy of the  $m_F = 0$  state is altered by this coupling, thus shifting the measured maser frequency in a carefully analyzed manner [31] described by a dispersive shape (Fig. 5(a)). Importantly, the maser frequency is unchanged when the driving field is exactly equal to the Zeeman frequency. Therefore, we determine the Zeeman frequency by measuring the driving field frequency at which the maser frequency in the presence of the driving field is equal to the unperturbed maser frequency.

The  $F = 1$ ,  $\Delta m_F = \pm 1$  Zeeman frequency is directly proportional to the static magnetic field, in the small-field limit. Four layers of high permeability ( $\mu$ -metal) magnetic shields surround the maser (Fig. 4), screening external field fluctuations by a factor of 32 000. Nevertheless, external magnetic field fluctuations cause remnant variations in the observed Zeeman frequency. As low frequency magnetic noise in the neighborhood of this experiment is much larger during the day than late at night, the measured Zeeman frequency could be preferentially shifted by this noise (at levels up to  $\sim 0.5$  Hz) with a 24 hour periodicity which is difficult to distinguish

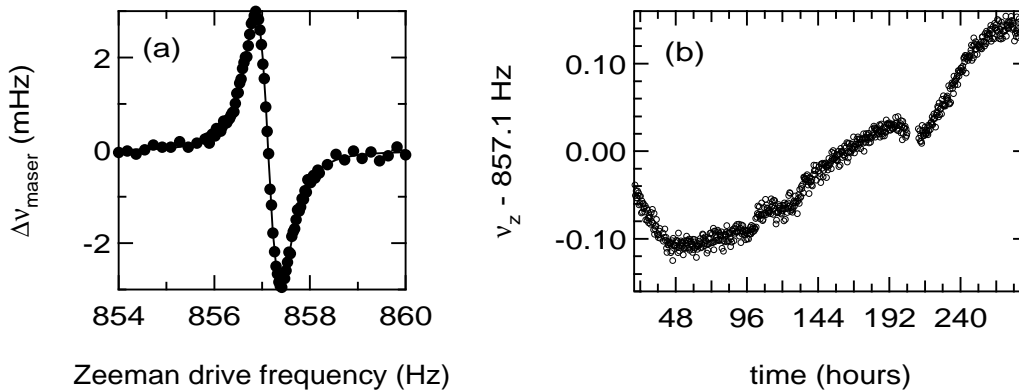


**FIGURE 5.** (a) An example of a double resonance measurement of the  $F = 1$ ,  $\Delta m_F = \pm 1$  Zeeman frequency in the hydrogen maser. The change from the unperturbed maser frequency is plotted versus the driving field frequency. (b) Zeeman frequency data from 11 days of the LLI/CPT test using the H maser.

from a true sidereal signal in our relatively short data sample. Therefore, we employ an active stabilization system to cancel such magnetic field fluctuations (Fig. 4). A fluxgate magnetometer placed as close to the maser cavity as possible controls large (2.4 m dia.) Helmholtz coils surrounding the maser via a feedback loop to maintain a constant ambient field. This feedback loop reduces the fluctuations at the sidereal frequency to below the equivalent of  $1 \mu\text{Hz}$  on the Zeeman frequency at the location of the magnetometer.

The Zeeman frequency of a hydrogen maser was measured for  $\sim 31$  days over the period Nov., 1999 to March, 2000. During data taking, the maser remained in a closed, temperature controlled room to reduce potential systematics from thermal drifts which might be expected to have 24 hour periodicities. The feedback system also maintained a constant ambient magnetic field. Each Zeeman measurement took approximately 20 minutes to acquire and was subsequently fit to extract a Zeeman frequency (Fig. 5(a)). Also monitored were maser amplitude, residual magnetic field fluctuation, ambient temperature, and current through the solenoidal coil which determines the Zeeman frequency (Fig. 4).

The data were then fit to extract the sidereal-period sinusoidal variation of the Zeeman frequency. (See Fig. 5(b) for an example of 11 days of data.) In addition to the sinusoid, piecewise linear terms (whose slopes were allowed to vary independently for each day) were used to model the slow remnant drift of the Zeeman frequency. No significant sidereal-day-period variation of the hydrogen  $F = 1$ ,  $\Delta m_F = \pm 1$  Zeeman frequency was observed. Our measurements set a bound on the magnitude of such a variation of  $\delta\nu_Z^H \leq 0.3 \text{ mHz}$ . Expressed in terms of energy, this is a shift in the Zeeman splitting of less than  $1 \cdot 10^{-27} \text{ GeV}$ .

The hydrogen atom is directly sensitive to LLI and CPT violations of the proton



and the electron. Following the notation of reference [14], one finds that a limit on a sidereal-day-period modulation of the Zeeman frequency ( $\delta\nu_Z^H$ ) provides a bound to the following parameters characterizing the magnitude of LLI/CPT violations in the standard model extension of Kostelecký and co-workers:

$$|b_3^e + b_3^p - d_{30}^e m_e - d_{30}^p m_p - H_{12}^e - H_{12}^p| \leq 2\pi\delta\nu_Z^H \quad (4)$$

for the low static magnetic fields at which we operate. (Again, we have taken  $\hbar = c = 1$ .) The terms  $b^e$  and  $b^p$  describe the strength of background tensor field couplings that violate CPT and LLI while the  $H$  and  $d$  terms describe couplings that violate LLI but not CPT [14]. The subscript 3 in Eqn. (4) indicates the direction along the quantization axis of the apparatus, which is vertical in the lab frame but rotates with respect to the fixed stars with the period of the sidereal day.

As in refs. [3,21], we can re-express the time varying change in the hydrogen Zeeman frequency in terms of parameters expressed in a non-rotating frame as

$$2\pi\delta\nu_{Z,J}^H = (\tilde{b}_J^p + \tilde{b}_J^e) \sin \chi. \quad (5)$$

where  $\tilde{b}_J^w = b_J^w - d_{j0}^w m_w - \frac{1}{2}\epsilon_{JKL}H_{KL}^w$ ,  $J = X, Y$  refers to non-rotating spatial indices in the plane perpendicular to the rotation vector of the earth,  $w$  refers to either the proton or electron parameters, and  $\chi = 42^\circ$  is the latitude of the experiment.

As noted above, a re-analysis by Adelberger, Gundlach, Heckel, and co-workers of existing data from the “Eöt-Wash II” spin-polarized torsion pendulum [23,24] sets the most stringent bound to date on CPT and LLI violation of the electron:  $\tilde{b}_J^e \leq 10^{-28}$  GeV [25]. Therefore, in the context of the standard model extension of Kostelecký and co-workers [14,3] the H maser measurement to date constrains LLI and CPT violations of the proton parameter  $\tilde{b}_J^p \leq 2 \cdot 10^{-27}$  GeV at the one sigma level. This limit is comparable to that derived from the  $^{199}\text{Hg}/^{133}\text{Cs}$  experiment of Lamoreaux, Hunter *et al.* [7,8] but in a much cleaner system (the hydrogen atom nucleus is a proton, compared to the complicated nuclei of  $^{199}\text{Hg}$  and  $^{133}\text{Cs}$ ).

## CONCLUSIONS

Precision comparisons of atomic clocks provide sensitive tests of Lorentz and CPT symmetries, thereby probing extensions to the standard model [3,9–17] in which these symmetries can be spontaneously broken. Measurements using the two-species  $^{129}\text{Xe}/^3\text{He}$  Zeeman maser constrain violations of CPT and Lorentz symmetry of the neutron at the  $10^{-31}$  GeV level. Measurements with atomic hydrogen masers provide clean tests of CPT and Lorentz symmetry violation of the proton at the  $10^{-27}$  GeV level. Improvements in both experiments are being pursued.

## ACKNOWLEDGMENTS

We gratefully acknowledge the encouragement and active support of these projects by Alan Kostelecký, and technical assistance by Marc Rosenberry and

Timothy Chupp. Development of the  $^{129}\text{Xe}/^3\text{He}$  Zeeman maser was supported by a NIST Precision Measurement Grant. Support for the Lorentz violation tests was provided by NASA grant NAG8-1434, ONR grant N00014-99-1-0501, and the Smithsonian Institution Scholarly Studies Program.

## REFERENCES

1. Will, C.M., *Theory and Experiment in Gravitational Physics*, Cambridge University Press, New York, 1981.
2. The discrete symmetries C, P, and T are discussed, for example, in Sachs, R.G., *The Physics of Time Reversal*, University of Chicago, Chicago, 1987.
3. Kostelecký, V.A., and Lane, C.D., *Phys. Rev. D* **60**, 116010/1-17 (1999).
4. Chupp, T.E., Hoare, R.J., Walsworth, R.L., and Wu, B., *Phys. Rev. Lett.* **72**, 2363-2366 (1994).
5. Stoner, R.E., Rosenberry, M.A., Wright, J.T., Chupp, T.E., Oteiza, E.R., and Walsworth, R.L., *Phys. Rev. Lett.* **77**, 3971-3974 (1996).
6. Bear, D., Chupp, T.E., Cooper, K., DeDeo, S., Rosenberry, M.A., Stoner, R.E., and Walsworth, R.L., *Phys. Rev. A* **57**, 5006-5008 (1998).
7. Berglund, C.J., Hunter, L.R., Krause, Jr., D., Prigge, E.O., Ronfeldt M.S., and Lamoreaux, S.K., *Phys. Rev. Lett.* **75**, 1879-1882 (1995).
8. Hunter, L.R., Berglund, C.J., Ronfeldt, M.S., Prigge, E.O., Krause, D., and Lamoreaux, S.K., "A Test of Local Lorentz Invariance Using Hg and Cs Magnetometers," in *CPT and Lorentz Symmetry*, edited by Kostelecký, V.A., World Scientific, Singapore, 1999, pp. 180-186.
9. Kostelecký, V.A., and Potting, R., "CPT, Strings, and the  $K - \bar{K}$  System," in *Gamma Ray-Neutrino Cosmology and Planck Scale Physics*, edited by Cline, D.B., World Scientific, Singapore, 1993, hep-th/9211116; *Phys. Rev. D* **51**, 3923-3935 (1995); Colladay D., and Kostelecký, V.A., *Phys. Lett. B* **344**, 259-265 (1995); *Phys. Rev. D* **52**, 6224-6230 (1995); Kostelecký, V.A., and Van Kooten, R., *Phys. Rev. D* **54**, 5585 (1996); Kostelecký, V.A., *Phys. Rev. Lett.* **80**, 1818-1821 (1998); *Phys. Rev. D* **61**, 16002/1-9 (2000).
10. Bluhm, R., Kostelecký, V.A., and Russell, N., *Phys. Rev. Lett.* **79**, 1432-1435 (1997); *Phys. Rev. D* **57**, 3932-3943 (1998).
11. Carroll, S.M., Field, G.B., and Jackiw, R., *Phys. Rev. D* **41**, 1231-1240 (1990).
12. Colladay, D., and Kostelecký, V.A., *Phys. Rev. D* **55**, 6760-6774 (1997); *ibid.* **58**, 116002/1-23 (1998); Jackiw, R., and Kostelecký, V.A., *Phys. Rev. Lett.* **82**, 3572-3575 (1999);
13. Bertolami, O., Colladay, D., Kostelecký, V.A., and Potting, R., *Phys. Lett. B* **395**, 178-183 (1997).
14. Bluhm, R., Kostelecký, V.A., and Russell, N., *Phys. Rev. Lett.* **82**, 2254-2257 (1999).
15. Bluhm, R., Kostelecký, V.A., and Lane, C.D., *Phys. Rev. Lett.* **84**, 1098-1101 (2000).
16. Bluhm, R. and Kostelecký, V.A., *Phys. Rev. Lett.* **84**, 1381-1384 (2000).
17. Coleman, S., and Glashow, S.L., *Phys. Rev. D* **56**, 116008/1-14 (1999).
18. Kostelecký, V.A. and Samuel, S., *Phys. Rev. D* **39**, 683-685 (1989); *ibid.* **40**, 1886-

- 1903 (1989); Kostelecký, V.A. and Potting, R., *Nucl. Phys. B* **359**, 545-570 (1991); *Phys. Lett. B* **381**, 89-96 (1996).
19. Kostelecký, V.A., and Samuel, S., *Phys. Rev. Lett.* **63**, 224-227 (1989); *ibid.* **66**, 1811-1814 (1991).
20. Gabrielse, G., Khabbaz, A., Hall, D.S., Heimenn, C., Kalinowski, H., and Jhe, W., *Phys. Rev. Lett.* **82**, 3198-3201 (1999).
21. Mittleman, R.K., Ioannou, I.I., Dehmelt, H.G., and Russell, N., *Phys. Rev. Lett.* **83**, 2116-2119 (1999).
22. Dehmelt, H., Mittleman, R., Van Dyck, Jr., R.S., and Schwinberg, P., *Phys. Rev. Lett.* **83**, 4694-4696 (1999).
23. Adelberger, E.G., *et al.*, in *Physics Beyond the Standard Model*, edited by P. Herczeg *et al.*, World Scientific, Singapore, 1999, p. 717.
24. Harris, M.G., Ph.D. thesis, Univ. of Washington, 1998.
25. Heckel, B., presented at International Conference on Orbis Scientiae 1999: Quantum Gravity, Generalized Theory of Gravitation and Superstring Theory Based Unification (28th Conference on High Energy Physics and Cosmology Since 1964), Fort Lauderdale, Florida, 16-19 Dec., 1999.
26. Walker, T.G., and Happer, W., *Rev. Mod. Phys.* **69**, 629-642 (1997).
27. Romalis, M.V., and Cates, G.D., *Phys. Rev. A* **58**, 3004-3011 (1998); Newbury, N.R., Barton, A.S., Bogorad, P., Cates, G.D., Mabuchi, H., and Saam, B., *Phys. Rev. A* **48**, 558-568 (1993); Schafer, S.R., Cates, G.D., Chien, T.R., Gonatas, D., Happer, W., and Walker, T.G., *Phys. Rev. A* **39**, 5613-5623 (1989).
28. We employed the F-test at the 99% confidence level to decide whether the addition of a new term to the fit model was justified. See Philip R. Bevington, *Data Reduction and Error Analysis for the Physical Sciences, Second Ed.*, McGraw-Hill, Boston, 1992, ch. 11.
29. Vessot, R.F.C., *et al.*, *Phys. Rev. Lett.* **45**, 2081-2084 (1980); Turneure, R.J.P., Will, C.M., Farrell, B.F., Mattison, E.M., and Vessot, R.F.C., *Phys. Rev. D* **27**, 1705-1714 (1983); Walsworth, R.L., Silvera, I.F., Mattison, E.M., and Vessot, R.F.C., *Phys. Rev. Lett.* **64**, 2599-2602 (1990).
30. Kleppner, D., Goldenberg, H.M., and Ramsey, N.F., *Phys. Rev.* **126**, 603-615 (1962); Kleppner, D., Berg, H.C., Crampton, S.B., Ramsey, N.F., Vessot, R.F.C., Peters, H.E., and Vanier, J., *Phys. Rev.* **138**, A972-983 (1965).
31. Andresen, H.G., *Z. Physik*, **210**, 113-141 (1968).